Parametric Study on Thermal Properties of a PMSM Motor in Cryogenic Environment Using COMSOL Multiphysics®

J. Tran*[1,2], J. González Cabrero[2], C. Mandla[2], M. Plattner[2], M. Zimmermann[1]
1. Laboratory of product development and lightweight design, Technical University of Munich, Munich, Germany
2. Max-Planck-Institute for extraterrestrial physics, Munich, Germany
*Corresponding author: jtran@mpe.mpg.de

Abstract
We are developing a Permanent Magnetic Synchronous Machine (PMSM) for being used inside a cryostat. This environment is characterized by ultra high vacuum (UHV) and operating temperatures down to 80 K. In order to optimize our current design, we have been performing a design study about the key parameters of the machine. One of the challenges that we were confronted with is the analysis of thermal behavior during operation of the motor. Its power consumption will generate heat and thermal gradients within the motor might change the performance. Therefore, the temperature profile inside the machine generated during operation has been analyzed and the results are shown in this paper. The objective is to find an ideal configuration for the PMSM with respect to heat generation and cooling during operation. A design optimization methodology has been developed using the COMSOL Multiphysics® Joule Heating physics. For a parametric study, electromagnetic properties are calculated in MATLAB® and implemented into the model using the respective LiveLink™.

Keywords: Electric Machines, PMSM, Cryogenics, Optimization, Structural Mechanics, COMSOL/MATLAB programming

Introduction

Motors are used in all kinds of applications as actuators for mechanisms. However, machine concepts for operation in cryogenic environment are still not conventional. Cold optics of telescope instruments are operated at a temperature of 77 K and in a depressurized environment in order to provide high SNR of optical detector read-out. With the common use of stepper motors, microvibrations are generated which can degrade the positioning and point performance and thereby the overall performance of the instrument. To overcome this intrinsic limitation of stepper motors, a synchronous machine has been designed that offers a much higher running smoothness. The design of this rotational PMSM with application for optical instruments is analyzed in this paper.

For a design of a PMSM in conceptual phase, parametric analysis is used to find the optimum geometry. The main design drivers for the motor are maximizing the torque and minimizing heat generation during operation while maintaining positioning accuracy in the µrad range. The defined requirements for the design parameters are listed in Table 1 below:

Table 1: Requirements of main design parameters

Parameter	Value
Diameter	$40 – 60\ mm$
Length	$30 – 50\ mm$
Nominal torque	$> 100\ mNm$
Mass	$< 500\ g$
Coil loss	$< 50\ mW$

The machine shall be thermally insulated from all heat sensitive objects as losses are still evident. The aim of the design is to keep the losses low and the torque high for operations in cryostats. Frictional and iron losses are neglected for this conceptual design. Therefore, the focus of this work will be the evaluation of heat generation of the motor during operation.

Analysis in COSMOL provide many methods for the design of the motor. Thermal, electromagnetic and structural analysis can be combined by multiphysics coupling. However, due to large computation effort for such a complex coupling an alternative approach is used for the sizing of the motor. With the help of MATLAB LiveLink connection to COMSOL a combined analysis of analytical electromagnetic calculations and numerical heat transfer is elaborated. By using parametric sweeps from MATLAB commands, the overall motor design remains flexible and can be easily adapted for any input parameters.

Motor

Concept

The motor concept is based on a PMSM with an air gap winding which has the advantage of a high power density. Furthermore, there is no current in the rotor which reduces

the required cooling power. The rotor position depends directly on the stator voltages (3 phases). This simplifies the positioning control. The conceptual model is shown in Figure 1.

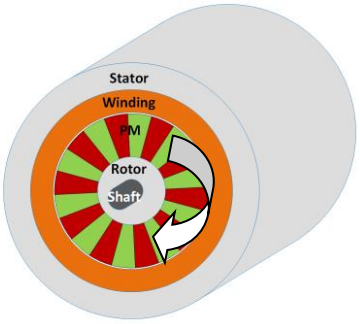

Figure 1. Concept of PMSM

The iron losses can be limited by low rotating speed of the machine and packaging of the stator with laminated sheets. To achieve a high positioning accuracy, the number of pole pairs was selected to eight. The air gap winding is kept in place by polymeric place holders.

Material selections

Materials for the motor have to be outgassing resistant as they will operate in UHV. Additionally, they should remain its properties at low temperatures. which is mainly an issue for the magnetic flux density of the permanent magnets. Due to missing convection in UHV, the rotor is only cooled by thermal radiation. Magnetic characteristics change with decreasing temperature. For permanent magnets the residual flux density B_R and the coercive field strength H_C increase with decreasing temperatures. That enhances the flux density in the air gap. The iron losses in rotor and stator increase as a result of a wider hysteresis curve as well.

Soft magnetic materials with high saturation flux density and no increased iron losses at cryogenic temperatures shall be used for the stator and rotor [1]. Neodymium-iron-boron permanent magnets are used because of good properties for power density of the machine. The winding shall transport high current with minimal losses. Due to the good thermal conductivity of copper at low temperatures, the winding material is copper. Insulating materials for the winding are neglected in the analysis. The relevant material properties used for analysis are listed in Table 2.

Table 2: Material properties

Soft Iron stator and rotor	
Residual flux density $\boldsymbol{B_R}$	1.5 T
Relative permeability μ	8000
Thermal conductivity $\boldsymbol{\lambda}$	30 $\frac{W}{mK}$
CTE $\boldsymbol{\alpha}$	9.4 *10^{-6} $\frac{1}{K}$
Yield strength $\boldsymbol{R_{p0,2}}$	250 MPa
Neodymiu-iron-boron magnets	
Relative permeability μ	1.1
Relative permittivity $\boldsymbol{\varepsilon_r}$	1
Thermal conductivity $\boldsymbol{\lambda}$	5 – 15 $\frac{W}{mK}$
CTE parallel $\boldsymbol{\alpha_{\parallel}}$	4 – 9 *10^{-6} $\frac{1}{K}$
CTE parallel $\boldsymbol{\alpha_{\perp}}$	-2 – 0 $\frac{1}{K}$
Flexural strength	240 MPa
Copper	
Thermal conductivity $\boldsymbol{\lambda}$	400 $\frac{W}{mK}$
Density $\boldsymbol{\rho}$	8.96 $\frac{g}{cm^3}$
CTE $\boldsymbol{\alpha}$	17 *10^{-6} $\frac{1}{K}$
Yield strength $\boldsymbol{R_{p0,2}}$	40 – 80 MPa

Winding Scheme

For the motor a linear stator winding is used. A distributed winding over the circumference is chosen for smooth running behavior. A parallel winding leads to a ripple-free constant torque. The winding has two layers and is short pitched. That means the first and second layer have the same width. The second layer is shifted by one slot with respect to the first layer. Therefore, the average coil width is not equal to the pole pitch. A wave winding for the winding heads is chosen due to greater resistance against mechanical stress. The winding scheme is depicted in Figure 2.

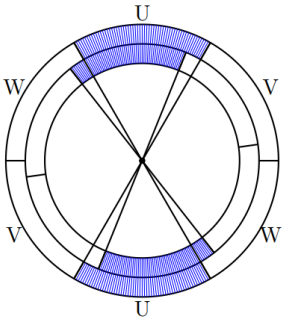

Figure 2. Short pitched winding scheme [2]

Baseline parameters

The baseline dimensions that have been defined for analysis are based on first analytical calculation. With the defined parameters the main requirements can be fulfilled. However, for further consideration of loss and torque optimization a parametric sweep is considered. Some of the baseline dimensions are listed in Table 3 and displayed in a section drawing in Figure 3.

Table 3: Baseline design parameters

Dimensions [mm]	
Inner bore diameter of stator $\boldsymbol{D}$	45
Height of stator $\boldsymbol{h_{St}}$	2.5

Air gap $\boldsymbol{\delta}$	0.5
Height of PMs $\boldsymbol{h_{PM}}$	7
Length of magnets $\boldsymbol{l}$	40
Height of rotor $\boldsymbol{h_{Rot}}$	3
Winding properties	
Phases $\boldsymbol{m}$	3
Wires per phase $\boldsymbol{q}$	4
Pole pair $\boldsymbol{p}$	8
Diameter of wire Ø [mm]	0.5

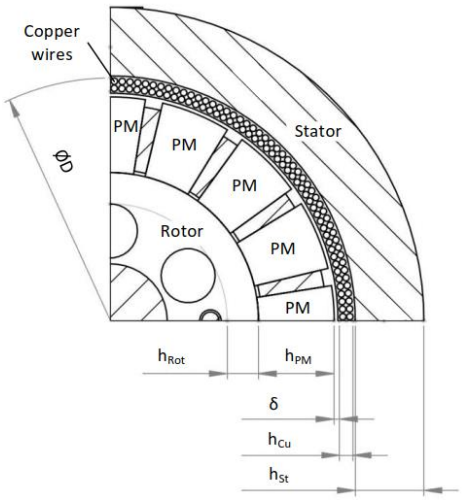

Figure 3. Illustration of baseline design parameters

With a rotating frequency of $f = 10\,Hz$ and with full utilization of copper losses a current of $500\,mA$ and a torque of approximately $130\,mNm$ is achieved. With this configuration the overall mass is estimated to be around $450\,g$.

Theory

The electromagnetic analysis which includes electric loading, magnetic circuit and winding scheme are performed analytically in MATLAB. The analytical calculations for the electromagnetic properties are based on following assumptions:

- Magnetic field is independent of the axial component.
- Eddy currents at the edges of the machine are neglected.
- Magnetic field in air gap is independent of the radius of the air gap.
- Permeability of the iron in stator and rotor is greater than one and constant.
- There is no unipolar field (e.g. by eccentric bearing of rotor).

The maximum torque of the electrical machine can then be defined as follows [3]:

$$M = \frac{\pi}{4}(D - h_{Cu})^2\, l\, A\, B_\delta$$

Where A is the electric loading and B_δ the flux density in the air gap. Since the geometrical dimensions D and l are limited, the torque primarily depends on the electric loading and the flux density in the air gap. The flux density in the air gap is given by:

$$B_\delta = -\mu_0 \frac{h_{PM}}{\delta + h_{Cu}}\left(H_{PM} - \frac{\theta}{h_{PM}}\right)$$

With μ_0 being the magnetic constant, H_{PM} the magnetic field strength of the permanent magnets (PM) and θ the magnetomotive force. From the equation it can be seen that the flux density depends on the field strength as well as on the height of the PMs.
The electric loading and copper losses are closely linked with the winding scheme. In case of a three-phase winding, the electric loading represents the total electric loading of all three phases over a pole pitch [4]:

$$A = \frac{3 * w * I}{p * \tau_p}$$

The number of pole pairs p and the pole pitch τ_p are fixed values from the machine design. The number of coils w results from the winding scheme. As each phase has the same number of coils, w for a double-layer winding is defined as follows [4]:

$$w = \frac{2 * n}{m}$$

Where m is the number of phases and N is the number of slots describing the parallel coils of all phases.
From the electric loading equation, it can be seen that the electric loading directly depends on the current. Then again, the current is related to the heat loss generated at maximum. And the main losses are represented by the copper losses which are defined as:

$$P_{Cu} = I^2 R = I^2 \rho \frac{l_{total}}{A_l} = I^2 \rho \frac{l\,(1 + l_{wk})\,w}{A_l}$$

With U as the voltage, I the current, R the resistivity of the winding and ρ the specific resistivity of copper. As l is the effective length of the machine, l_{wk} is defined as the length of the winding heads per l. l_{wk} is assumed to be

25% of l. A_l is the cross-section area of the coils and can be calculated by using the slot fill ratio.
The iron losses consist of hysteresis and eddy currents losses. The hysteresis loss is defined by:

$$P_{Hyst} = k \frac{4\,H_C}{\rho} B_{max}\, f$$

Where k is a constant close to $k \approx 1$, f is the frequency, ρ the density of the material, H_C is the coercive field strength and B the flux density. It should be noted that both H_C and ρ increase at decreasing temperature. The eddy current losses are given by:

$$P_W = \frac{\pi^2\,\sigma\,d^2}{6\,\rho} {B_{max}}^2\, f^2$$

Where d is the thickness and σ is the specific conductivity of the tested material. It should be noted that ρ increases, meanwhile d decreases at liquid nitrogen temperature. By using these formulas and the material properties for stator iron and permanent magnets, calculations show that the losses for permanent magnets are by the order of 10^{-4} smaller than iron and coil losses. Therefore, they are neglected for the heat analysis.

Modelling Method

For the heat analysis of the motor a COMSOL multiphysics model is set up. The heat sources of the PMSM itself are the previously described heat losses of the motor during operation. The coil and stator eddy current losses are most significant. Therefore, only these losses are considered.

The thermal time scale is usually larger than the time variation of the eddy current losses. Therefore, separating the electromagnetic and thermal simulation is necessary for computational efficiency. The heating powers are calculated analytically by a MATLAB routine using simplified electromagnetic formulation. By nested functions which describe the electric loading, magnetic circuit and winding scheme, the losses for stator and coil are derived. With the LiveLink functionality different load cases can be set in a routine script by changing parameter sets for each case. This simplifies the overall process which is controlled by the script. The overall analysis process is illustrated in Figure 4.

In COMSOL the heating is modelled by electric currents, heat transfer in solids, radiation as well as solid mechanics in order to retrieve deformation and stresses. These domains are coupled by multiphysics of electromagnetic heating, heat transfer with radiation, thermal expansion and temperature coupling. The COMSOL server is controlled by MATLAB LiveLink which also sends the datasets back for post-processing of the results.

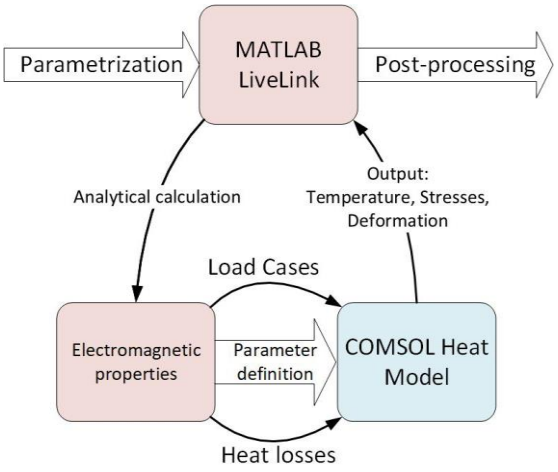

Figure 4. Analysis process

For the parametric sweep, a preliminary sensitivity analysis has been considered. The analysis is based only on the electromagnetic calculations in MATLAB. The main concern for the motor is the component temperature during operation. For the electromagnetic domain the parameters torque M_{max} as well as the current density S are the target figures. As depicted in the bar diagram displayed in Figure 5, it can be seen that the target figures S and M_{max} are mostly influenced by D and p. Hence, these are varied in the COMSOL parametric study for thermal loads. The electromagnetic target functions will not be further covered in heat analysis.

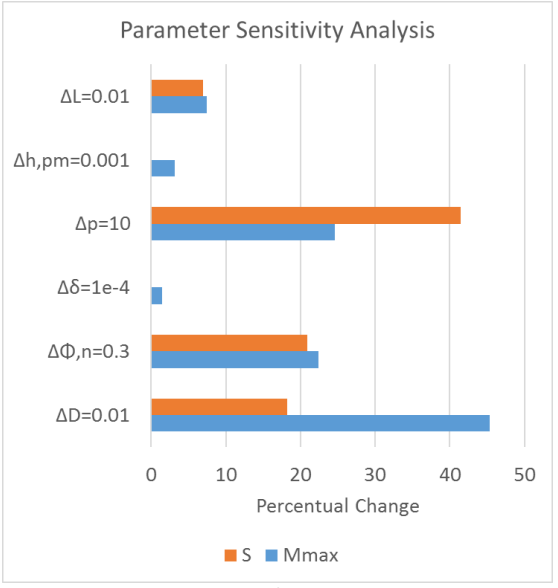

Figure 5. Sensitivity analysis for parameter sweep

In order to get the temperature distribution over the volume a 3D model is created. However, the motor is built as a 3D section in order to reduce the computational effort. Sector symmetry and axial mirror symmetry is then applied.

Simulation Results

For the parametric analysis two load cases are considered. As the motor is applied in cryogenic environment, a stationary heat analysis considers the temperature distribution for long-term operation times and a time-dependent analysis considers the temperature after a typical operation time of 10 minutes. For both analysis, initial as well as ambient temperature is at 77 K and the ambient pressure at 10^{-8} bar. The parameter sweep for D is based on defined requirements listed in Table 1. The sweep parameters are summarized in Table 4. A total of 30 versions are analyzed within one sweep.

Table 4: Sweep parameter definition

Sweep parameters	
$\boldsymbol{D}$	[40, 45, 50, 55, 60]
$\boldsymbol{p}$	[4, 6, 8, 10, 12]

When looking at the resulting heat losses of coil and stator for all variants in Figure 6, one can see that the losses increase for smaller diameters D and higher number pole pair magnets p. This is expected, as from the torque and electric loading equations a proportionality for p and losses P and an antiproportionality for D and P can be concluded.

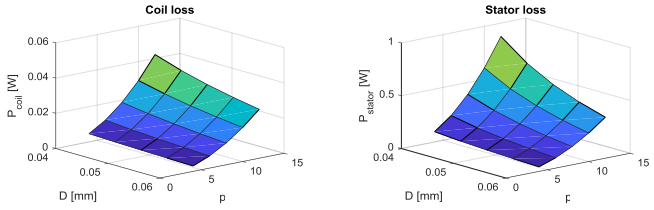

Figure 6. Losses of the motor for all configurations

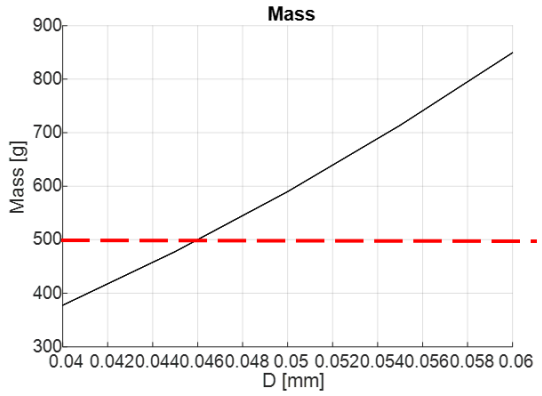

Figure 7. Diameter to mass dependency

The diameter has more influence on the overall motor mass than the pole pairs. The mass and diameter dependency is shown in the graph of Figure 7. With the requirement defined in Table 1, a limitation for the diameter can be set at approximately 46 mm.

Stationary

The computation of the stationary behavior shows the temperature distribution when the motor is operated within a time where temperature equilibrium is achieved. Figure 8 shows the achieved maximum temperature for rotor, stator and coil of all combinations. A higher temperature is present when the diameter is smaller and the pole pairs is higher which makes sense according to the heat loss distribution shown in Figure 6.

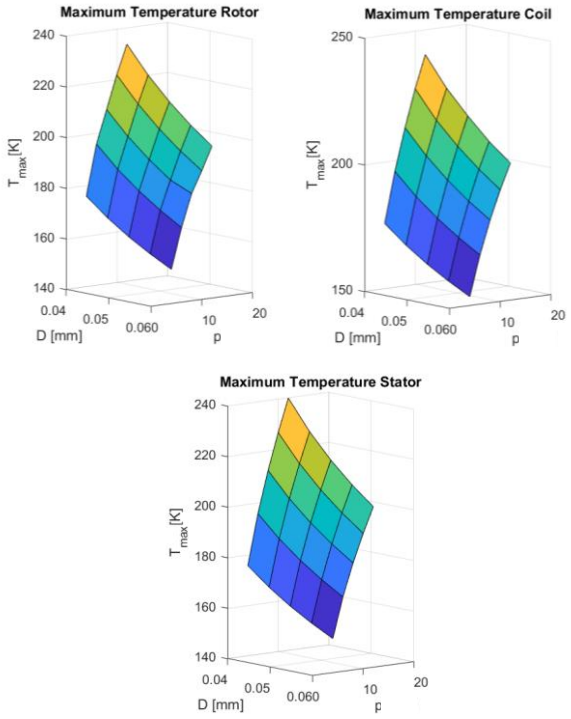

Figure 8. Maximum temperatures of all configurations

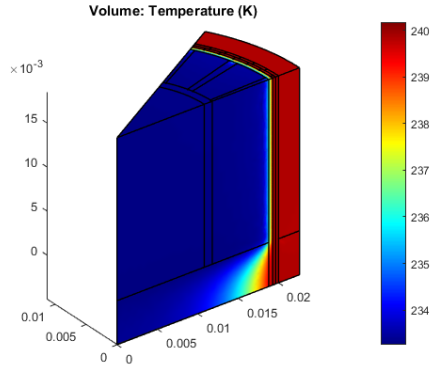

Figure 9. Temperature distribution for stationary analysis of motor section with worst case of D = 40 mm and p = 12

The coil temperature is a little higher than the temperatures in rotor and stator which is due to higher coil losses. The maximum temperature in the coil for the worst combination is at 240 K. The corresponding plot for temperature distribution is shown in Figure 9 where the blue area represents 230 K and the red are the

maximum temperature. It can be seen that stator and coil show the highest temperature.

Time-dependent

The time-dependent study is set to a typical operation time of 10 min and is calculated in a 2 s step. The temperature rise is shown in Figure 10 after a time of 600 s. Due to high computational load the resolution for the parametric study is lowered for this case. The maximum temperature is achieved for the coil and the stator. For both components a ΔT of approximately 9 K is achieved. For the rotor only a ΔT of 2 K is achieved. The rotor temperature difference shows a highest value at pole pair of 8. This is not expected as with larger diameter the temperature usually decreases. This phenomenon has to be analyzed with a higher resolution.

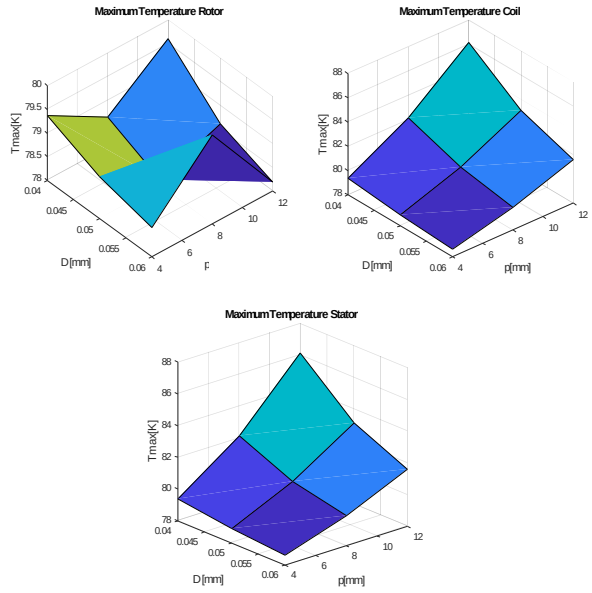

Figure 10. Temperature rise for rot coil and stator at t = 600 s

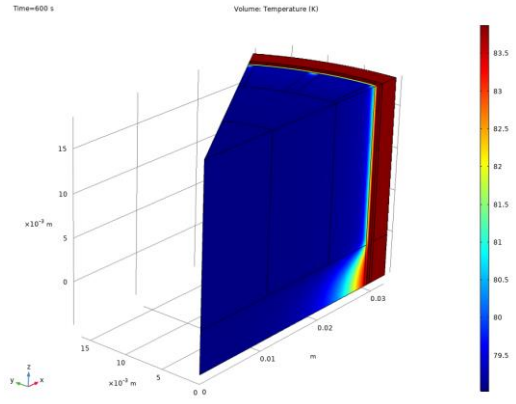

Figure 11. Temperature distribution for time-dependent analysis of motor section with D = 60 mm and p = 12 at t = 600 s

The general temperature distribution of a rotor section after a limited time is displayed in Figure 11 for the case of D = 60 mm and p = 12. It can be seen that the temperature difference within the motor is only in the range of 6 K. The coil shows the higher temperature due to its high heat loss coming from small material section area.

Cooling down process

With the optimal configuration for least heat generation of the motor a further case is considered which is the cooling down process from room temperature (RT) to cryogenic temperature. During the cooling down process the deformation and stresses are of interest. For that, the stresses and deformations are evaluated as well. Both results are illustrated in Figure 12 and 13.

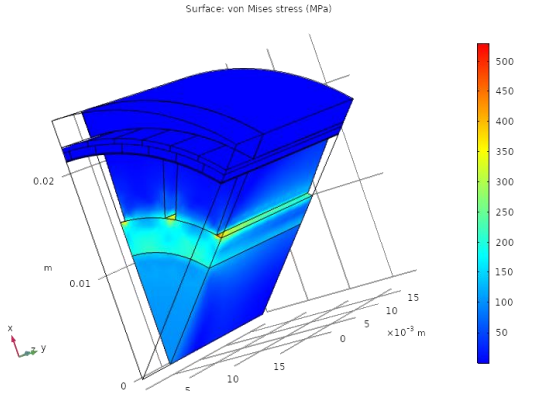

Figure 12. Stress distribution after cooling down process for optimal configuration

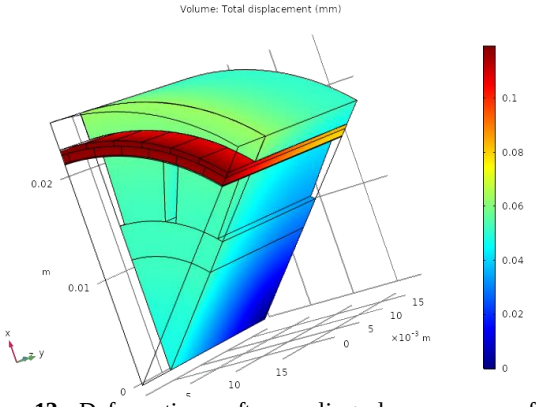

Figure 13. Deformations after cooling down process for optimal configuration

The stresses show a maximum value between magnets and rotor. A maximum stress of 500 MPa surpasses the material yield strength properties. This can be further optimized by material or geometry modification.
The maximum deformation after the cooling down process is 0.1 mm which is smaller than the defined air gap of 0.5 mm. The coil deforms most due to higher temperature gradients. Therefore, the deformation is acceptable for this design.

Conclusions

For the design of an electrical machine a parametric study has been performed. With the help of MATLAB LiveLink functionality of COMSOL a methodology for easy parameter definition and load case control by parameter change within a script has been established. The mathematical model of the motor has been defined in MATLAB and the electromagnetic heat losses are passed to a heat transfer model in COMSOL. For post-processing the results are sent back to MATLAB. The linked analysis routine can be used for flexible design optimization.

The analysis method has been used on the application of a PMSM. For that, two significant parameters have been varied, the outer diameter D and the number of pole pairs p. The temperature distribution is analyzed for 30 configurations with combined parameters within one sweep. A maximum temperature map could be evaluated for stationary as well as time-dependent analysis of 10 min. It can be concluded that more heat is generated for smaller diameters and higher number of magnetic pole pairs. The proportionality between heat losses and temperature rise can be confirmed. The typical operation time of 10 min shows an optimum temperature gradient of 6 K with a coil deformation of 0.14 mm which still enables the air gap.

For the optimum configuration which resulted from the optimization routing ($D = 60\,mm$, $p = 12$), the cooling down process has been analyzed regarding stresses and deformations. The stresses between magnets and rotor are beyond the material yield strength limits whereas the deformations are rather small. For improvement of stresses, optimization regarding material as well as geometrical parameters can be further performed using the established methodology by defining respective design variables.

References

1. P. Breining, M. Veigel, M. Doppelbauer, Y. Liu, M. Noe, *Iron Loss Measurement of Nonoriented Silicon and Cobalt Iron Electrical Steel Sheets at Liquid Nitrogen Temperature Using Ring Specimen*, *Journal*, 2017 IEEE International Electric Machines and Drives Conference (IEMDC).
2. F. Heiles, *Wicklungen elektrischer Maschinen und ihre Herstellung*. 2nd ed. Berlin, Göttingen, Heidelberg: Springer, 1953.
3. G. Müller, B. Ponick. *Theorie elektrischer Maschinen*. 6th ed. Weinheim: Wiley-VCH, 2009.
4. G. Müller, K. Vogt, B. Ponick. *Berechnung elektrischer Maschinen*. 6th ed. Weinheim: Wiley-VCH, 2008.